

## EAR INFECTION

## Detecting middle ear fluid using smartphones

Justin Chan<sup>1\*†</sup>, Sharat Raju<sup>2,3\*†</sup>, Rajalakshmi Nandakumar<sup>1</sup>,  
Randall Bly<sup>2,3</sup>, Shyamnath Gollakota<sup>1†</sup>Copyright © 2019  
The Authors, some  
rights reserved;  
exclusive licensee  
American Association  
for the Advancement  
of Science. No claim  
to original U.S.  
Government Works

The presence of middle ear fluid is a key diagnostic marker for two of the most common pediatric ear diseases: acute otitis media and otitis media with effusion. We present an accessible solution that uses speakers and microphones within existing smartphones to detect middle ear fluid by assessing eardrum mobility. We conducted a clinical study on 98 patient ears at a pediatric surgical center. Using leave-one-out cross-validation to estimate performance on unseen data, we obtained an area under the curve (AUC) of 0.898 for the smartphone-based machine learning algorithm. In comparison, commercial acoustic reflectometry, which requires custom hardware, achieved an AUC of 0.776. Furthermore, we achieved 85% sensitivity and 82% specificity, comparable to published performance measures for tympanometry and pneumatic otoscopy. Similar results were obtained when testing across multiple smartphone platforms. Parents of pediatric patients ( $n = 25$  ears) demonstrated similar performance to trained clinicians when using the smartphone-based system. These results demonstrate the potential for a smartphone to be a low-barrier and effective screening tool for detecting the presence of middle ear fluid.

## INTRODUCTION

The presence of middle ear fluid is the key diagnostic marker for the two most common pediatric ear diseases, acute otitis media (AOM) and otitis media with effusion (OME) (1). AOM, known commonly as an “ear infection,” is characterized by the presence of infected fluid in the middle ear and results in symptoms of fever and ear pain. It is a leading cause of pediatric healthcare visits, and although many cases can resolve without antibiotics, complications may include eardrum perforation, mastoiditis, facial nerve palsy, or meningitis (2–4). OME is the presence of middle ear fluid without signs of an acute infection and affects up to 80% of children (5, 6). Although OME has few overt symptoms, making diagnosis more difficult, it is associated with speech delay, sleep disruption, poor school performance, balance issues, and a higher likelihood of developing AOM (5).

Diagnosis of OME or AOM requires detecting middle ear fluid using either pneumatic otoscopy or tympanometry (1). Pneumatic otoscopy is used by only 7 to 33% of primary care providers and is not designed for home screening purposes (5). Tympanometry necessitates a referral to an audiologist and the use of expensive equipment (7, 8). For these reasons, in 2016, the American Academy of Otolaryngology called for research into a brief, reliable, and objective method to detect middle ear fluid as well as new in-home strategies to help parents and caregivers monitor fluid after initial physician evaluation (5).

Here, we describe a system that uses the microphone and speaker of existing smartphones to detect middle ear fluid by assessing eardrum mobility. The system sends a soft acoustic chirp into the ear canal using the smartphone speaker, detects reflected sound from the eardrum using the smartphone microphone, and uses a logistic regression machine learning model to classify these reflections

and predict middle ear fluid status. No additional attachments are required beyond a paper funnel, which acts as a speculum and can be constructed from printer paper, scissors, and tape. Real-time implementation and data processing are performed entirely on the smartphone, compatible with both iPhone and Android devices. The system demonstrated comparable performance across multiple smartphone platforms and when used by parents versus clinicians. Given the ubiquity of smartphones, this system may hold potential as a middle ear screening tool for parents as well as health care providers in resource-limited regions.

## RESULTS

## Concept and prototype

Our system uses the smartphone speaker to play audible, 150-ms frequency-modulated continuous wave chirps from 1.8 to 4.4 kHz into the patient’s ear canal. The microphone remains active during the chirp, collecting both incident waves from the speaker and reflected waves from the eardrum. Sound reflected from the eardrum will destructively interfere with the incident chirp, causing a dip in sound pressure along a range of frequencies. A normal eardrum resonates well at multiple sound frequencies, creating a broad-spectrum, soft echo; as a result, the shape of the resulting acoustic dip is broad and shallow in the frequency domain. In contrast, a fluid or pus-filled middle ear, as found in OME and AOM, restricts the vibrational capacity of the eardrum; sound energy that would have vibrated the eardrum is instead reflected back along the ear canal, creating more destructive interference and resulting in a narrower and deeper acoustic dip. The acoustic dip occurs at the resonant frequency of the ear canal where the quarter-wavelength of the chirp is equal to the length of the canal (9). Thus, although individual differences in ear canal length affect the location of the dip along the frequency domain, the shape of the dip primarily depends on eardrum mobility.

Our system builds upon existing acoustic reflectometry methods in three ways (10–14). First, it is a predominantly software-based solution that takes advantage of existing smartphone hardware rather than requiring a separate device. Current acoustic reflectometers

<sup>1</sup>Paul G. Allen School of Computer Science & Engineering, University of Washington, Seattle, WA 98195, USA. <sup>2</sup>Department of Otolaryngology—Head and Neck Surgery, University of Washington, Seattle, WA 98195, USA. <sup>3</sup>Seattle Children’s Hospital and Research Institute, Seattle, WA 98105, USA.

\*These authors contributed equally to this work.

†Corresponding author. Email: jucha@uw.edu (J.C.); sraju@uw.edu (S.R.); gshyam@uw.edu (S.G.)

require a microphone and speaker in close proximity to produce and measure sound waves along the ear canal. Many modern smartphones have a similar configuration, with a co-located speaker and microphone on their bottom edge for noise cancellation (Fig. 1A). This includes all versions of iPhone, Samsung Galaxy phones after the S5, and other Android phones, including the Google Pixel. Second, we use a paper funnel as a speculum to direct sound into the ear canal. The funnel (Fig. 1B) can be assembled using a printed paper template (fig. S1), scissors, and tape. Without this attachment, the resulting waveform can be highly variable because sound could reflect off of different structures of the pinnae. Third, the system uses a logistic regression machine learning model to classify the waveforms received by the microphone. To identify whether a patient has middle ear fluid, we first preprocessed the raw waveform to locate and isolate the acoustic dip (Fig. 1, C and D). We then used logistic regression to determine whether the shape of the dip was more indicative of a normal or fluid-filled ear. A text-based message is presented to the user indicating a result: “suggestive of middle ear fluid” or “middle ear fluid unlikely” (fig. S2). On an iPhone 5s and Galaxy S6, data processing and classification took 771.98 ms and 1.2 s, respectively.

### Clinical testing

We tested system performance for detecting middle ear fluid in two separate cohorts. First, we conducted a clinical study on patients between 18 months and 17 years of age. We used this population to train the algorithm and obtain cross-validated performance

measures. Second, we recruited a separate cohort of patients under 18 months of age and evaluated performance using the algorithm trained in the first clinical study.

The first clinical study was conducted at Seattle Children’s Hospital surgical centers using a cohort of 98 patient ears between 18 months and 17 years of age from two different subgroups: patients undergoing ear tube placement, a common surgery performed on patients with chronic OME or recurrent AOM ( $n = 48$  ears), and patients undergoing a different surgery, such as a tonsillectomy, with no recent symptoms of AOM or OME and no signs of middle ear fluid by physical examination ( $n = 50$  ears). The median age of recruited patients was 5.0 [interquartile range (IQR), 2.0] years, height was 113.2 (IQR, 19.0) cm, weight was 20.0 (IQR, 9.2) kg, and the female-to-male ratio was 0.6 (table S1).

A trained clinician performed all patient testing in a private waiting room just before surgery and with the patient awake and held or sitting upright (movie S1). Soft chirps were played into the ear canal using multiple smartphone models and a new paper funnel for each patient. All patients were also tested in parallel with commercial acoustic reflectometry hardware (7, 12, 15). After surgery, we prospectively assigned each ear its actual middle ear fluid status. A patient was considered positive for middle ear fluid if, during ear tube placement, an incision into the eardrum (myringotomy) yielded fluid ( $n = 24$ ) or if the patient had a red, bulging eardrum consistent with AOM ( $n = 2$ ). A patient was considered negative for middle ear fluid if, during ear tube placement, myringotomy yielded no fluid ( $n = 24$ ) or if the patient did not receive ear tubes, did not

have ear-related symptoms, and was negative for fluid on pneumatic otoscopy performed by the otolaryngologist ( $n = 48$ ).

For classification, we used a logistic regression algorithm on pre-processed microphone acoustic data. The sound intensity (in decibels) of each frequency along the acoustic dip was inputted as a separate feature. The algorithm was trained with iPhone 5s data collected from patients. Its classification accuracy was evaluated with leave-one-out cross-validation (LOOCV), a rigorous method to validate machine learning models (16). During each iteration of LOOCV, 97 of 98 patient ears are used to train a model that is then used to output a prediction for the remaining one patient ear. This process is repeated for all 98 ears to estimate the accuracy of a model trained on all 98 ears when tested on unseen data. A receiver-operating characteristic (ROC) curve was generated from the cross-validation step with an area under the curve (AUC) of 0.898 (Fig. 2A). The operating point was chosen to have an overall sensitivity and specificity of 84.6% [95%

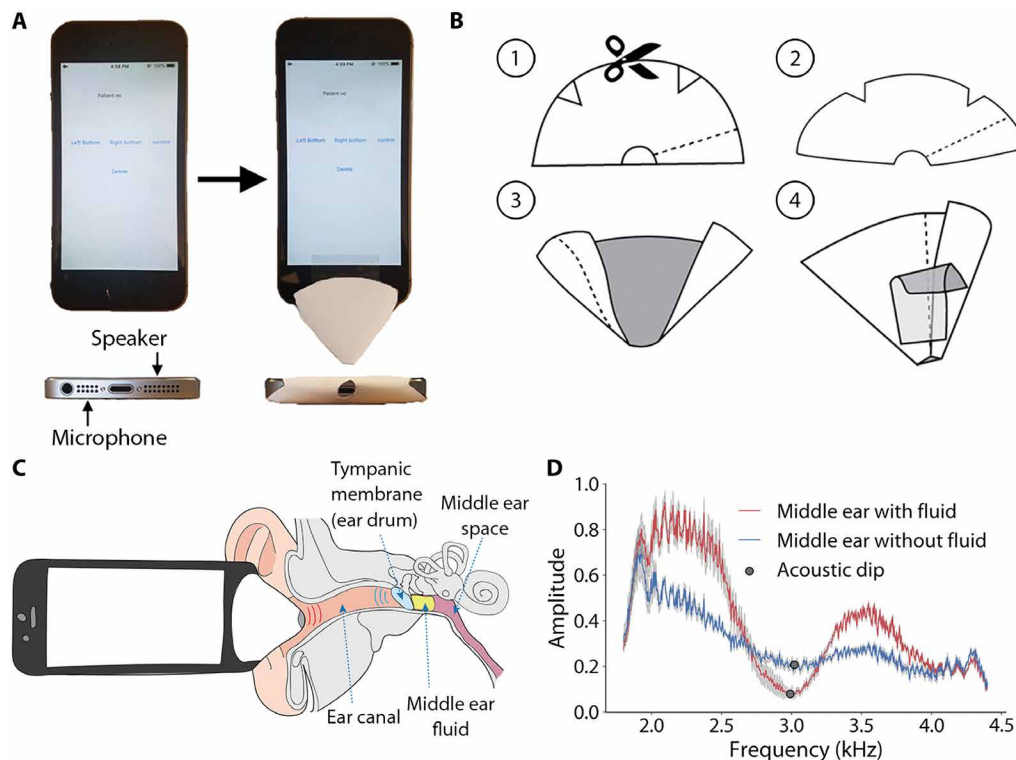


**Fig. 1. Using a smartphone to detect middle ear fluid.** (A) Location of speaker and microphone on the bottom of an iPhone 5s, without and with paper funnel attached. (B) Process of assembling smartphone funnel. (C) Proper placement of smartphone and funnel at ear canal entrance. (D) Raw acoustic waveform obtained when chirps are played into an ear with middle ear fluid (red) and without fluid (blue). The SD (gray) is computed across 10 chirp instances on a patient's ear.

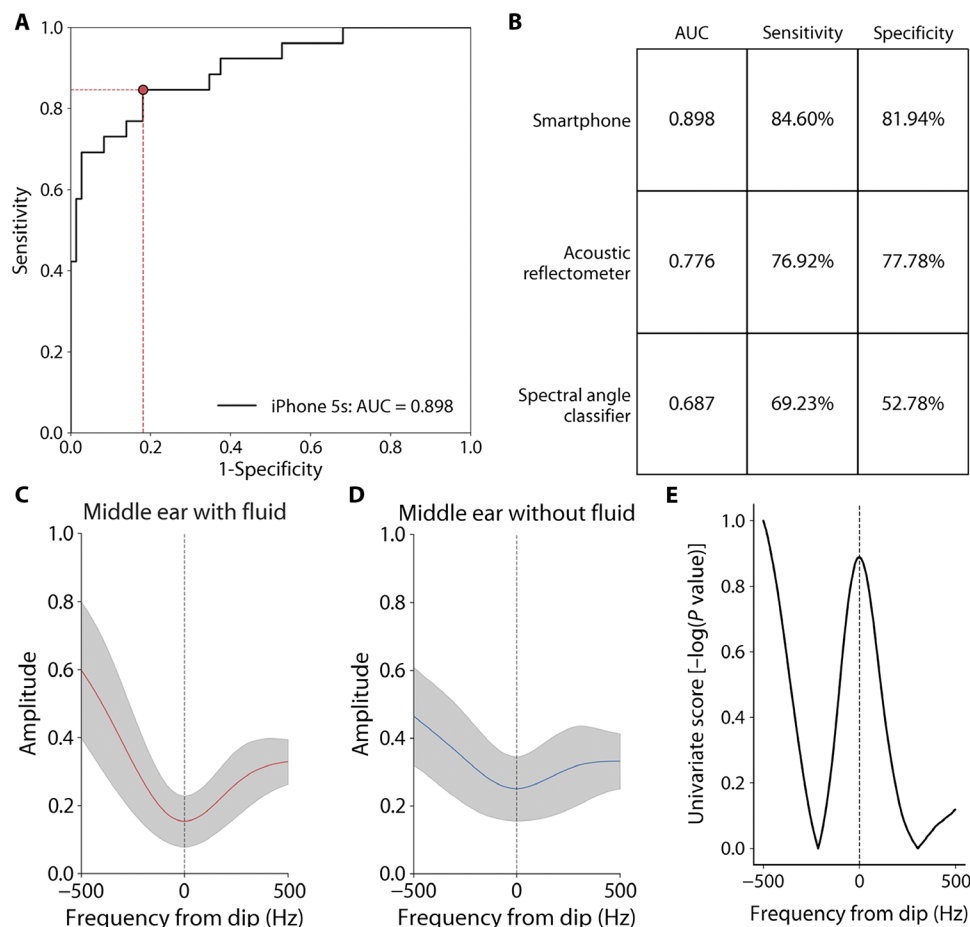


**Fig. 2. Classification of patient ears from clinical testing.** (A) ROC curve for our middle ear fluid detection algorithm, cross-validated on data collected from patients using an iPhone 5s ( $n = 98$ ), with operating point denoted by the red circle. (B) Comparison of performance for smartphone-based detection, acoustic reflectometry, and spectral angle-only classification during parallel clinical testing ( $n = 98$ ). (C and D) Mean acoustic dip classified by the algorithm as with middle ear fluid (red) and without middle ear fluid (blue). Shaded region represents one SD from the mean. (E) Feature analysis indicating the weight that the classifier places on each frequency around the acoustic dip.

confidence interval (CI), 65.1 to 95.6%] and 81.9% (95% CI, 71.1 to 90.0%), respectively. With  $k$ -fold ( $k = 10$ ) cross-validation (17), we obtained a comparable AUC of 0.906. To address potential bias from training on the same patient's opposite ear, we repeated LOOCV, but during each iteration, we also excluded the contralateral ear from the training set, achieving an AUC of 0.899. We also downsampled the frequency response curve to 100 samples and obtained a similar AUC of 0.888. The fluid type was recorded as either being serous ( $n = 7$ ), mucoid ( $n = 11$ ), or purulent ( $n = 4$ ) for 22 of 36 ears that had middle ear fluid. The algorithm correctly classified 86% (6 of 7) of ears that had serous fluid, 91% (10 of 11) of ears with mucoid fluid, and 100% (4 of 4) of ears with purulent fluid. These estimates predict the real-world clinical performance on unseen data of our final algorithm, which is trained on all 98 ears from the iPhone 5s dataset (Fig. 2B). Across male patients, for the iPhone 5s, 15 of 17 positive ears and 31 of 40 negative ears were classified correctly. Across female patients, 7 of 9 positive ears and 25 of 30 negative ears were classified correctly. For two ears, we did not record gender.

Post hoc, we examined how the algorithm classified acoustic waveforms. Figure 2 (C and D) plots the mean sound intensities at

each frequency for all ears classified by the model. The algorithm predicted that ears with narrower and deeper acoustic dips were more likely to have middle ear fluid. Similarly, on univariate analysis, sound intensities at the top and bottom of the waveform, which determine the depth of an acoustic dip, were given the most weight by the predictive model (Fig. 2E). This result indicates that the algorithm can independently identify an acoustic pattern for middle ear fluid that is consistent with the known acoustic response of the eardrum (7, 12, 15).

The smartphone-based system demonstrated improved clinical performance compared to acoustic reflectometry (18), which uses custom hardware to assess middle ear fluid status. Head-to-head testing (Fig. 2B) across the 98 patient ears demonstrated an AUC of 0.898 for the smartphone-based approach compared to an AUC of 0.776 for commercial acoustic reflectometry (EarCheck Middle Ear Monitor, Innovia Medical). The smartphone algorithm's improved clinical performance may be the result of applying machine learning over the waveform rather than relying on the hand-selected features used by acoustic reflectometers (7). When classifying patient waveforms obtained from smartphones, we found that using only the spectral angle, as described in previous literature (7), reduces the AUC to 0.687.

We evaluated test-retest reliability in the pediatric patients enrolled in our clinical study. Each ear was tested twice per smartphone; between each attempt, the

funnel was fully removed from the ear and reinserted. Of the 66 ears tested twice, 94% of the ears were classified the same between each attempt. When a discrepancy occurred, the algorithm used the positive result to minimize false negatives. Each testing attempt consisted of 10 chirps, and we tested the consistency across these chirps. In the clinical study, 93 of 98 ears showed no difference in classification among all 10 chirps. When doing a majority vote across the first three chirps, 96 of 98 ears showed no difference in classification compared to using a single chirp. Across all 98 ears, there was no difference when considering the classification result to be the majority (more than 5) of the 10 chirps (table S2).

Last, using the algorithm trained in the first study, we evaluated the system's performance in a separate cohort of patients under 18 months of age to assess accuracy in a younger population. We again recruited surgical patients at Seattle Children's Hospital, using the same criteria described in the first study with the exception of age. This cohort included 15 patient ears and had a median age of 1.1 (IQR, 0.3) years, height of 76.0 (IQR, 7.8) cm, weight of 9.3 (IQR, 2.1) kg, and female-to-male ratio of 1.5 (Fig. 3A). The lowest age among this cohort was 9 months. All 5 ears that were positive for

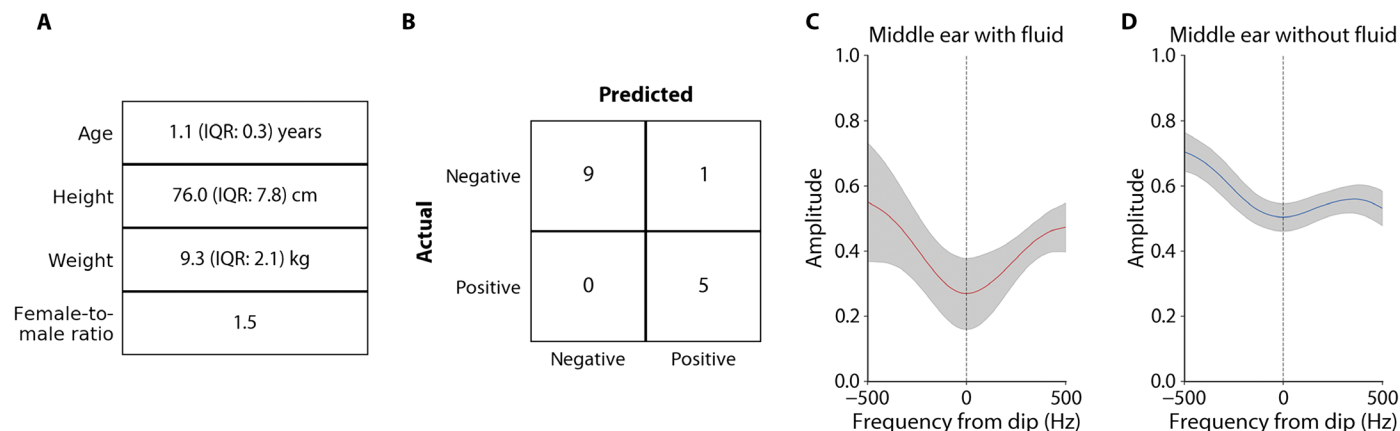


**Fig. 3. Classification of patient ears under 18 months.** (A) Demographic table of patients under 18 months. (B) Confusion matrix of the algorithm's performance for patients under 18 months. (C and D) Mean acoustic dip of ears of patients under 18 months ( $n = 15$ ) classified by the algorithm as with middle ear fluid (red) and without fluid (blue). Shaded region represents one SD from the mean.

fluid and 9 of 10 ears that were negative for fluid were classified correctly (Fig. 3B). The shape of the acoustic dips paralleled those in the first clinical study: Ears with fluid had a deeper and narrower acoustic dip compared to ears without fluid (Fig. 3, C and D, and fig. S3). This shows that an algorithm trained on patients over 18 months of age can properly classify patients under 18 months. We also trained and tested our algorithm's performance when using patients under 18 months as the training cohort. When running LOOCV across the 15 patient ears that were under 18 months of age, 5 of 5 ears positive for fluid and 10 of 10 ears negative for fluid were correctly classified. This is similar to the performance of the algorithm that is trained on the 98 patient ears over 18 months of age.

### Performance across other mobile platforms

All patients in the first cohort ( $n = 98$  ears) were tested in parallel with both the iPhone 5s and the Samsung Galaxy S6. Using LOOCV, we estimated performance of the iPhone 5s-trained system on unseen Galaxy S6 data. Specifically, the entire iPhone 5s dataset was used for training except for one patient ear, which was "held out" for testing. The trained algorithm was then tested on Galaxy S6 data from the held-out ear. This was repeated for all patient ears in the cohort to generate an AUC of 0.851, as shown in Fig. 4A. In the same manner, we also tested a subset of this cohort using an iPhone 6s ( $n = 10$  ears), Samsung Galaxy S7 ( $n = 12$ ), and Google Pixel ( $n = 8$ ). The algorithm correctly classified 80% (8 of 10) of iPhone 6s data, 91.7% (11 of 12) of Galaxy S7 data, and 83.3% (7 of 8) of Pixel data (Fig. 4B). The low sample size in these subgroups precluded generation of meaningful AUC values. Processed waveforms for a given test ear across phone models are shown in fig. S4, and waveforms for the remaining test ears are shown in fig. S5.

### Performance testing with nonclinicians

In a clinical setting, we evaluated the system's performance when used by parents. Trained clinicians briefly demonstrated proper technique for testing, and the parent of a pediatric study participant subsequently performed unaided testing on their child. The parent's results were then compared to those of the trained clinician. This cohort included 25 patient ears and had a median age of 4.0 (IQR, 6.0) years, height of 105.0 (IQR, 38.1) cm, weight of 16.4 (IQR, 13.9) kg, and female-to-male ratio of 1.1 (Fig. 5A). All 6 ears positive for fluid

were classified the same by clinicians and parents, and 18 of 19 ears negative for fluid were classified the same (Fig. 5B). In addition, the mean acoustic dip was similar between clinicians (red) and parents (black) (Fig. 5, C and D). Individual curves for each patient are shown in fig. S6.

We tested the usability of funnel construction with a separate cohort of 10 untrained adults. After playing a short instructional video (see movie S2), we first measured the time it took participants to create and mount the funnel using a paper template, tape, and scissors. The average time was 2.8 ( $\pm 0.93$ ) min. We then queried participants about the usability of the entire system; they gave an average usability rating of 8.9 ( $\pm 1.1$ ) on a scale of 1 (unusable) to 10 (extremely usable) (table S3).

### Effect of confounding ear pathologies

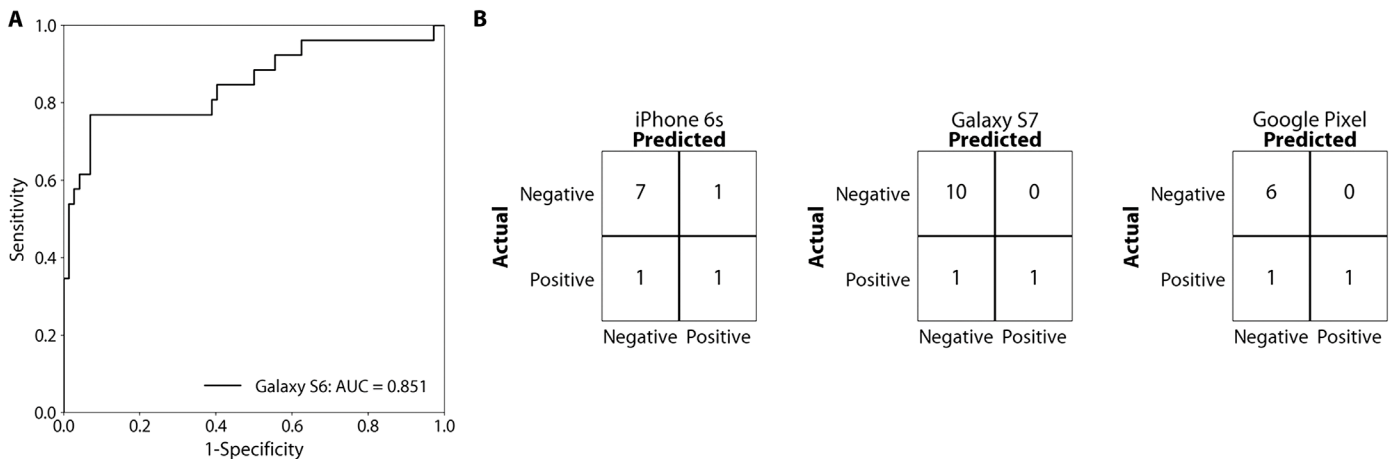
In the above studies, we exclude patients with ear pathologies that affect eardrum mobility. Next, we evaluated the algorithm's performance in the presence of ear pathologies such as cholesteatoma ( $n = 1$ ), ossicular chain discontinuity ( $n = 1$ ), acute eardrum inflammation ( $n = 1$ ), and previous tympanoplasty surgery ( $n = 3$ ) (fig. S7). The algorithm produced false positives for middle ear fluid in all these patients.

Similarly, patients undergoing myringotomy but lacking middle ear fluid may have abnormal middle ear pressure that can affect eardrum mobility. In our cohort, there were seven patients reported by the surgeon as having acutely inflamed eardrums. Only one of these patients presented without fluid on myringotomy. This patient's ear was classified as positive by the algorithm (fig. S7). Thus, in the event that a patient presents with an inflamed eardrum but has not yet developed middle ear fluid, the algorithm would likely test positive and appropriately prompt further evaluation. The other acutely inflamed eardrums ( $n = 6$  ears) had middle ear fluid and were appropriately classified as positive by the algorithm.

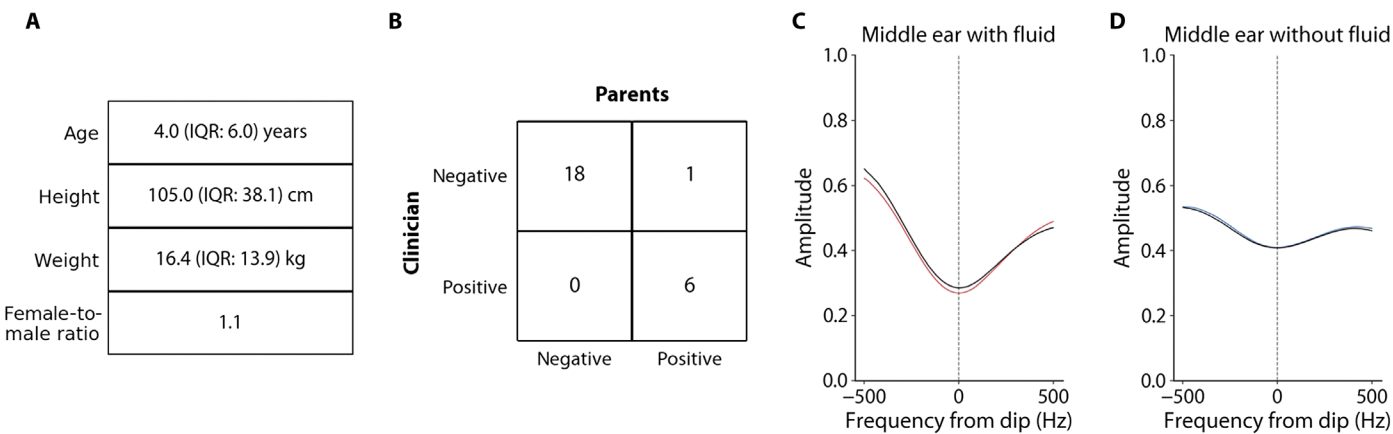
### Benchmark testing

Figure 6 demonstrates benchmark performance of our smartphone-based system across various design and environmental conditions. We identified design and environmental conditions that could affect system accuracy, including background noise, incident angle of the smartphone, alterations to the funnel, and changes in chirp volume. Testing was performed with a 2.5-cm closed-ended plastic





**Fig. 4. Classification performance across other mobile platforms.** (A) ROC curve for our middle ear fluid detection algorithm, cross-validated on data collected from patients using a Samsung Galaxy S6 ( $n = 98$ ). (B) Confusion matrices comparing performance on three other smartphones.



**Fig. 5. Performance testing with trained clinicians versus untrained parents.** (A) Demographic table of patients that were tested by parents. (B) Confusion matrix of the algorithm's performance for patient ears ( $n = 25$ ) tested by parents. (C and D) Mean acoustic dip of ears tested by parents (black) and clinicians classified by the algorithm as with middle ear fluid (red) and without fluid (blue).

tube used to calibrate existing acoustic reflectometers as a positive control (19). The hard-backed end of the tube reflects sound to produce a narrow and deep acoustic dip that mimics an ear with middle ear effusion.

First, we used four different paper types of varying thickness and consistency to construct the funnel: filler paper, inkjet paper, laserjet paper, and cardstock. Changing paper type did not affect the classification accuracy (Fig. 6A). We also tested whether changes to tip opening diameter affected accuracy. The funnel is designed to have a tip opening diameter of 7 mm to approximate the diameter of the ear canal (20). Variations in tip diameter from 5 to 10 mm did not affect performance. However, diameters of 1 and 3 mm produced false negatives (Fig. 6B). This suggests that a tip opening diameter between 5 and 10 mm is required.

Second, we varied the incident angle of our smartphone with respect to the calibration tube to examine the system's performance with slight deviations from direct line of sight. The smartphone tolerated up to a 45° offset from line of sight (Fig. 6C). Offsets of 60 or 75° produced a less prominent dip and false negatives. This suggests that while a parallel orientation is ideal, the system has some

tolerance for non-ideal positioning. To validate the benchmark testing, we evaluated the effect of angle of insertion in an upright patient (16 months of age) with middle ear fluid confirmed on myringotomy. To accurately assess angle of insertion, we used the built-in smartphone gyroscope to measure smartphone rotation. Initially, the smartphone was placed in line with the axis of the ear canal and began playing and recording chirps. Angular data were recorded for each chirp while the phone was rotated up (positive) and down (negative), up to 30° off axis. All chirps were correctly classified as positive within this range (fig. S8). Different insertion angles are also accounted for during clinical testing, where there was natural variance in measurement angle.

Third, we examined whether changes in background sound affected device accuracy, particularly with a crying child. We used an external speaker to play an audio file of a baby crying, with an average volume from 80 to 110 dBA. We tested our system in the calibration tube when it was placed directly next to the speaker (within 2 cm). In a measurement attempt, where five chirps were played, most of the chirps were correctly classified across tested volume levels during three different measurement attempts (Fig. 6D).

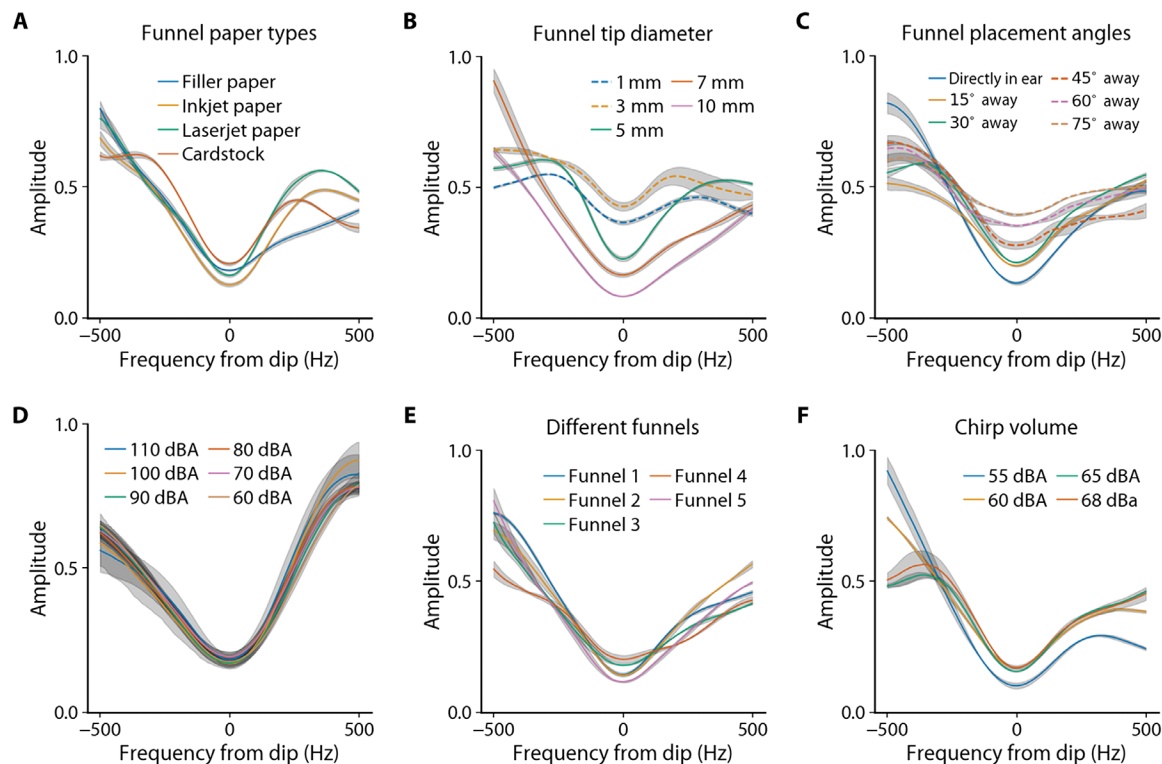


**Fig. 6. Benchmark testing across different scenarios.** (A) Different paper types used to construct the funnel. (B) Different tip diameters of the funnel. (C) Different funnel placement angles. (D) Different background noise (infant crying) intensities. (E) Funnels created by different individuals. (F) Different chirp volumes. Solid and dashed lines indicate conditions where the algorithm classifies the waveform correctly and incorrectly, respectively. The figure shows the mean for each test and an SD computed across five chirp instances.

When the background volume was lower than 80 dBA, all chirps were correctly classified. In the clinical study, there was no substantial background noise. We report data on the ear of a 2-year-old patient who was crying and had partial motion of the head. Figure S9 shows the mean and the SD of the processed chirps used by our algorithm; this validates our benchmark testing on the effect of environmental noise.

Fourth, we tested the effect of deforming the funnel on classification of waveforms when using the calibration tube as a positive control. No deformation and partial deformation (more severe than typical use), as demonstrated in fig. S10, were appropriately classified as positive. Full deformation resulted in a false negative. Our clinical study had variance in funnel deformation among different users and ears, and thus, the clinical results account for slight variations during actual use. We also tested the effect of different funnel instances on classification accuracy. Five different untrained users were instructed to construct a funnel and test it on the positive control. All acoustic curves were correctly classified as a positive ear (Fig. 6E). We also varied the sound intensity of chirps from 55 to 68 dBA. We found no difference in classification of the positive control (Fig. 6F).

Last, we consider the presence of cerumen (ear wax) and its effects on system performance. Our patients had partial cerumen occlusion (range, 0 to 50%) as estimated by the surgeon; our data indicate that this did not impair the algorithm's performance. Because none of our patients had complete cerumen occlusion, we used a positive control calibration tube for further testing. As expected, playing chirps into the tube generated a deep and narrow

acoustic dip. Using putty to mimic cerumen, we found that partially occluding wax (60 to 70%) had little effect on the shape or position of the dip, as shown in fig. S11A. This is consistent with previous observations that acoustic-based techniques are unaffected by less than 50% cerumen occlusion (21). In contrast, 100% cerumen occlusion, also known as impaction, occurs in 10% of children (22) and alters the waveform substantially. As the site of impaction moves closer to the entrance of the ear canal, the acoustic dip appears shallower and occurs at a higher frequency due to an effectively shorter canal and corresponding quarter-wavelength, as shown in fig. S11B. In these cases, chirps can reflect off cerumen, generating a false acoustic dip that does not reflect middle ear status. For example, at a depth of 1 cm, which is the deepest point cerumen would naturally accumulate (23), our tests produced a false acoustic dip located about 1 kHz higher compared to a normal dip from eardrum reflections. At shallower depths of impaction, the false dip was even more right-shifted. Impaction at the entrance produced a waveform similar to calibration chirps played into open air (fig. S11C). Given that the mean acoustic dip in our patients was located at 3 kHz (range, 2.4 to 3.7 kHz), a cerumen detection system in future prototypes could include an error display if an acoustic dip is identified outside the normal range or if the waveform resembles an in-air calibration chirp. Such a system must acknowledge that cotton swab insertion or iatrogenic manipulation can result in cerumen impaction deeper than 1 cm. These findings suggest that partial occlusion does not affect results, and full occlusion can be readily identified.

## DISCUSSION

Proper diagnosis of AOM and OME requires an examination of middle ear fluid status (1, 5). Currently, most assessments of middle ear fluid are made either in primary care clinics and urgent care centers or, in recent years, remotely using smartphone-attached otoscopes (24–27). These assessments can be costly and time consuming. Furthermore, they usually rely on visual information without an assessment of eardrum mobility, which can compromise accuracy because middle ear fluid often produces only subtle changes in the eardrum's appearance (28–30). Techniques that assess eardrum mobility, such as pneumatic otoscopy and tympanometry, have high sensitivity and specificity (90 and 80% for specialist-performed pneumatic otoscopy) but are infrequently performed outside of a specialist's office (31). Other methodologies, such as air-coupled ultrasound, short-wave infrared imaging, and optical coherence tomography, hold promise in terms of accuracy, but they require additional specialized and expensive hardware (32–34). Thus, there is a need for a middle ear fluid screening technique that does not use costly equipment or attachments, can evaluate eardrum mobility, and requires minimal expertise.

The value of a low cost, smartphone-based screening tool lies in its accessibility and user familiarity. Ninety-six percent of all parents we queried regarding potential participation in the study consented, and many were interested in learning more about the technology. Although some children were apprehensive before the study, the phone's chirps (which sound like a small bird) had a calming effect, causing many children to respond with smiles or laughs.

Our system has several limitations. As with many screening tools, interpretation of the results requires appropriate clinical context such as symptoms and time course, and positive results should prompt further clinical evaluation for potential misclassifications. This system also does not distinguish between different types of middle ear fluid (purulent, serous, or mucoid). Knowing fluid type could potentially be useful for identifying AOM versus OME, although this distinction is also made on the basis of clinical history and symptoms. Furthermore, as with most middle ear assessment techniques, the system requires that a child not be agitated and remain relatively still for the duration of testing: The algorithm needs a minimum of three chirps for reliable results, which takes 1.2 s; considerable head movement during this duration can cause interchirp inconsistency.

This smartphone-based screening tool relies on an evaluation of eardrum mobility to detect middle ear fluid. This is also true for tympanometry and pneumatic otoscopy, which are the screening techniques recommended by the American Academy of Pediatrics and American Academy of Otolaryngology for middle ear fluid detection. Ear pathologies that affect eardrum mobility, such as cholesteatoma, ossicular chain discontinuity, acute eardrum inflammation, and previous tympanoplasty surgery, can produce false positives for middle ear fluid. Similarly, patients undergoing myringotomy but lacking middle ear fluid may have abnormal middle ear pressure that can affect eardrum mobility. Despite the potential for false positives, the use of eardrum mobility to predict middle ear effusion is well established both in active clinical practice and in previous large-scale pediatric studies (35). Furthermore, in the context of screening, these false positives would appropriately prompt additional evaluation.

In summary, we present a proof-of-concept screening tool that can be implemented on commodity smartphones to determine the

presence of middle ear fluid. Given the ubiquity of smartphones, the system we describe may have clinically relevant applications in developing countries and rural communities where smartphone availability is rapidly growing, in primary care settings as an adjunct to visual otoscopy, or for home screening by parents as a platform to reduce health care costs. Further longitudinal clinical trials are required to determine the technology's impact in these and other potential scenarios.

## MATERIALS AND METHODS

### Study design

Our study was approved by the University of Washington and the Seattle Children's Hospital Institutional Review Boards. For our first clinical study ( $n = 98$  ears), we included otolaryngology patients undergoing surgery who were between the ages of 18 months and 17 years. Our second clinical study ( $n = 15$  ears) included otolaryngology surgical patients who were between 9 and 18 months of age. For both studies, we excluded patients with existing tympanostomy tubes, existing eardrum perforations, previous tympanoplasty, or known comorbid middle ear pathology, such as cholesteatoma or ossicular chain abnormalities. We stopped recruitment after a sufficient number of patient data were collected to demonstrate proof of concept. Randomization was not applicable. Surgeons were blinded to the results of preoperative smartphone testing.

### Smartphone application

Two custom applications—for iPhone and Android smartphones—were developed to emit chirps with a frequency range of 1.8 to 4.4 kHz, each for a duration of 150 ms. Each chirp was interspersed with 250 ms of silence. The smartphone simultaneously recorded audio from the microphone at a sampling rate of 48 kHz, the highest sampling rate possible on the smartphones tested.

### Data preprocessing

Our processing pipeline was implemented on an iPhone 5s and a Samsung Galaxy S6. Each chirp had 7200 samples and was padded with trailing zeros, so the total number of samples was 48,000. A 48,000-point fast Fourier transform (FFT) was then performed to capture the acoustic frequency response within a range of 0 to 24 kHz; we discarded frequencies outside the 1.8- to 4.4-kHz range of the transmitted chirp. This frequency range was chosen on the basis of literature in acoustic reflectometry (36). Except when evaluating retest and interchirp reliability, waveforms that were two or more SDs from the mean of other recorded chirp waveforms within a given attempt were excluded from analysis. Of the remaining chirps, we selected the second chirp for further processing. To reduce the variability caused by different funnels as well as microphone and speaker differences across devices, a calibration chirp was performed away from the ear and normalized to a unit frequency response to produce a set of weights. These weights were then used to normalize chirps captured in a subject's ear canal.

We then applied a moving average filter with a window size of 300 samples to smooth the waveform. Next, we used a peak detection algorithm to identify the acoustic dip. Specifically, the algorithm identified the most prominent dip within a range of 2.3 to 3.8 kHz. Looking for dips within the full range of 1.8 to 4.4 kHz resulted in no change in AUC for the iPhone 5s. After the dip was identified, we selected frequencies within 500 Hz of the dip for further processing.

This allows the machine learning algorithm to focus only on portions of the acoustic response that are most predictive of middle ear effusion status. Selecting frequencies within 600, 700, 800, 900, and 1000 Hz of the dip caused small ( $<0.02$ ) AUC changes for the iPhone 5s.

### Machine learning classifier

Our logistic regression classifier is computationally inexpensive and can run inferences on mobile devices. The frequency response for each ear was represented as an array of 1000 floating point values, where each element represents the amplitude for each of the 1000 selected frequencies around the acoustic dip. Each chirp was aggregated into a single matrix. Using a logistic regression machine learning model with an L2 penalty, we performed LOOCV to validate the discriminative accuracy of the algorithm on our dataset of 98 ears collected with the iPhone 5s. We also performed  $k$ -fold ( $k = 10$ ) cross-validation.

The classifier trained the model on the entire set of ears except for one. Testing was then performed on the omitted ear. This was repeated for all ears, and the overall accuracy was computed across all predictions. When computing predictions for the Samsung Galaxy S6 and other benchmark phones, we followed a similar LOOCV approach. We trained the algorithm on all ears from the iPhone 5s dataset except for one ear collected on the other device. The classifier then made a prediction on the omitted ear. This method evaluated whether the classifier can generalize to unseen ears on other devices.

The feature analysis in Fig. 3E was generated in sklearn using the SelectPercentile method, which calculates the analysis of variance (ANOVA)  $F$  value between each feature and the ground truth label. The spectral gradient angle of the acoustic dip in Fig. 3B was generated using reference points 200 Hz around the dip. The angles were trained and validated using LOOCV using a logistic regression classifier to obtain an AUC. Briefly, spectral gradient angle is the measurement used by existing acoustic reflectometers to determine the presence of middle ear fluid. It is computed as the angle between the slopes of the acoustic dip.

### Funnel design

The funnel was fabricated using printer paper and clear tape. A template for the funnel was designed using Adobe Photoshop and printed onto paper (fig. S1). The funnel was placed over a smartphone's speaker and microphone, and a small piece of tape attached it to the front and back. Each smartphone model required a customized funnel template optimized to envelope the speaker and microphone. The base of the funnel cone varied in size depending on the combined length and separation of the speaker and microphone. The funnel's base had a diameter of 45 mm for the Samsung Galaxy S6 and S7, 52 mm for the iPhone 5s, and 57 mm for the iPhone 6s and Google Pixel. For each template, the funnel was designed with a 7-mm-diameter opening, which approximates the size of the opening into the ear canal (20). Not every smartphone has ideal positioning of the microphone and speaker. To increase accessibility, we began prototyping a detection system using earbud headphones with a paper funnel (fig. S12). Further patient studies are needed to validate this approach.

### Clinical study design

We tested each patient's ear using a smartphone fitted with a paper funnel. Each phone had an installed application that played 10 identical chirps and simultaneously recorded the reflected echoes. We standardized the volumes for each phone to an average of

65 dBA. After attaching the funnel to our testing device, we played calibration chirps into the air, away from the patient. When the patient arrived, they were positioned upright for testing, either being held on their parent's lap or sitting in a chair.

The phone was placed near the child's ear, with the funnel positioned at the entrance to the ear canal. The ideal position for the funnel in most children was medial to the tragus, pointing medially and slightly anteriorly into the ear canal. In most cases, the canal was also straightened during testing by gently pulling the pinnae posteriorly. After playing the first set of chirps, the smartphone was withdrawn from the ear and repositioned in approximately the same location to produce a second set of chirps for reliability testing. This process was repeated for each phone and each ear. After device testing, we tested each ear with a U.S. Food and Drug Administration–approved acoustic reflectometry instrument (18, 19) and documented the ordinal output score on a scale from 1 to 5. We reclassified these outputs in accordance with previous studies (37): 1 and 2 results were classified as a normal ear, and 3 to 5 indicated an infected ear. Last, a subset of patients, particularly those not undergoing tympanostomy tube placement, underwent otoscopy to provide additional evidence regarding middle ear fluid status.

### Performance testing with nonclinicians

Our usability study ( $n = 25$  ears) included both otolaryngology surgery and clinic patients between 9 months and 17 years of age. As with the other clinical studies, we excluded patients with existing tympanostomy tubes, existing eardrum perforations, previous tympanoplasty, or known comorbid middle ear pathology such as cholesteatoma or ossicular chain abnormalities.

Clinicians demonstrated proper ergonomic positioning and placement of the smartphone system with respect to the ear canal. Proper device use included first pressing the record button, then directing the funnel tip medially and slightly anteriorly at the entrance to the ear canal, and finally pulling the pinnae posteriorly with the opposite hand. Patients were directed to wait until the chirps were finished playing before removing the device. After the clinician performed testing, parents were allowed to experiment with device placement for about 30 s to 1 min. After this period, parents performed actual unaided testing, which was recorded. We performed all usability testing on the Samsung Galaxy S6.

For funnel construction testing, we made an instructional video. Subjects were instructed to watch the video and subsequently construct the funnel, unaided, using the provided paper template, scissors, and tape. After construction and smartphone mounting, subjects were asked to rate the overall usability.

### Run-time analysis

Implementation on an iPhone was performed in Swift, and the Accelerate framework was used to perform FFTs. Android implementation was done in Java, and the JTransforms library was used to perform FFTs. On an iPhone 5s, data processing and classification took 771.98 ms, including 2.71 ms for dip detection, 0.06 ms for logistic regression, and 767.24 ms for 10 FFTs. On a Galaxy S6, the total runtime was 1.2 s, including 4.96 ms for dip detection, 0.67 ms for logistic regression, and 1200 ms for 10 FFTs.

### Statistical analysis

To obtain clinical performance metrics and perform cross-validation, the FFT, filtering, and peak detection were performed in MATLAB. NumPy



and scikit-learn were used to perform logistic regression, ROC analysis, and the calculation of accuracy, sensitivity, specificity, and 95% CI values. Line charts were created using matplotlib and seaborn.

## SUPPLEMENTARY MATERIALS

stm.sciencemag.org/cgi/content/full/11/492/eaav1102/DC1

Fig. S1. Funnel template for smartphone.

Fig. S2. Conceptual diagram of the smartphone-based system.

Fig. S3. Processed waveforms of patients under 18 months of age.

Fig. S4. Comparison of waveforms from an ear across different smartphones.

Fig. S5. Individual patient waveforms obtained from different smartphones.

Fig. S6. Processed waveforms of testing by parents.

Fig. S7. Processed waveforms of confounding ear pathologies.

Fig. S8. Effect of angle of insertion on system performance in a patient with middle ear fluid.

Fig. S9. Processed waveforms for a crying 2-year-old patient with partial head movement.

Fig. S10. Effect of funnel deformation on system performance.

Fig. S11. Effect of cerumen on acoustic waveforms.

Fig. S12. Design for earbud headphones.

Table S1. Demographic summary for first clinical study.

Table S2. Interchirp reliability testing.

Table S3. Funnel construction times and usability ratings.

Movie S1. Video illustrating proper technique for testing.

Movie S2. Instructional video for funnel construction.

## REFERENCES AND NOTES

- A. S. Lieberthal, A. E. Carroll, T. Chonmaitree, T. G. Ganiats, A. Hoberman, M. A. Jackson, M. D. Joffe, D. T. Miller, R. M. Rosenfeld, X. D. Sevilla, R. H. Schwartz, P. A. Thomas, D. E. Tunkel, The diagnosis and management of acute otitis media. *Pediatrics* **131**, e964–e999 (2013).
- D. Bowyer, *Complications of Otitis Media* (CRC Press, 2015).
- J. Acuin, *Chronic Suppurative Otitis Media: Burden of Illness and Management Options* (World Health Organization, 2004).
- A. Qureshi, Y. Lee, K. Belfield, J. P. Birchall, M. Daniel, Update on otitis media—Prevention and treatment. *Infect. Drug Resist.* **7**, 15–24 (2014).
- R. M. Rosenfeld, J. J. Shin, S. R. Schwartz, R. Coggins, L. Gagnon, J. M. Hackell, D. Hoelting, L. L. Hunter, A. W. Kummer, S. C. Payne, D. S. Poe, M. Veling, P. M. Vila, S. A. Walsh, M. D. Corrigan, Clinical practice guideline: Otitis media with effusion (update). *Otolaryngol. Head Neck Surg.* **154**, S1–S41 (2016).
- I. Williamson, Otitis media with effusion in children. *BMJ Clin. Evid.* **2015**, 0502 (2015).
- H. Lindén, H. Teppo, M. Revonta, Spectral gradient acoustic reflectometry in the diagnosis of middle-ear fluid in children. *Eur. Arch. Otorhinolaryngol.* **264**, 477–481 (2007).
- J. Lous, Why use tympanometry in general practice: A review. *World J. Otorhinolaryngol.* **5**, 53–57 (2015).
- E. A. Shaw, R. Teranishi, Sound pressure generated in an external-ear replica and real human ears by a nearby point source. *J. Acoust. Soc. Am.* **44**, 240–249 (1968).
- D. W. Teele, J. Teele, Detection of middle ear effusion by acoustic reflectometry. *J. Pediatr.* **104**, 832–838 (1984).
- R. M. Lampe, M. R. Weir, J. Spier, M. F. Rhodes, Acoustic reflectometry in the detection of middle ear effusion. *Pediatrics* **76**, 75–78 (1985).
- J. T. Combs, M. K. Combs, Acoustic reflectometry: Spectral analysis and the conductive hearing loss of otitis media. *Pediatr. Infect. Dis. J.* **15**, 683–686 (1996).
- J. Chianese, A. Hoberman, J. L. Paradise, D. K. Kolborn, D. Kearney, H. E. Rockette, M. Kurs-Lasky, Spectral gradient acoustic reflectometry compared with tympanometry in diagnosing middle ear effusion in children aged 6 to 24 months. *Arch. Pediatr. Adolesc. Med.* **161**, 884–888 (2007).
- T. Muderris, A. Yazıcı, S. Bercin, G. Yalçın, E. Sevil, M. Kins, Consumer acoustic reflectometry: Accuracy in diagnosis of otitis media with effusion in children. *Int. J. Pediatr. Otorhinolaryngol.* **77**, 1771–1774 (2013).
- S. Kimball, Acoustic reflectometry: Spectral gradient analysis for improved detection of middle ear effusion in children. *Pediatr. Infect. Dis. J.* **17**, 552–555 (1998).
- M. Kearns, D. Ron, Algorithmic stability and sanity-check bounds for leave-one-out cross-validation. *Neural Comput.* **11**, 1427–1453 (1999).
- S. Rose, Machine learning for prediction in electronic health data. *JAMA Intern. Med.* **1**, e181404 (2018).
- Innovia Medical, Lenexa, KS, Earcheck middle ear monitor (2018).
- Innovia Medical, Lenexa, KS, Earcheck middle ear monitor use & care manual.
- D. D. Mahoney, W. P. Sjørnsen, W. J. Staab, M. Leedom, One-size-fits-all uni-ear hearing instrument. U.S. Patent 7,092,543 (2006).
- S. L. Block, E. Mandel, S. McLinn, M. E. Pichichero, S. Bernstein, S. Kimball, J. Kozikowski, Spectral gradient acoustic reflectometry for the detection of middle ear effusion by pediatricians and parents. *Pediatr. Infect. Dis. J.* **17**, 560–564 (1998).
- D. F. McCarter, A. U. Courtney, S. M. Pollart, Cerumen impaction. *Am. Fam. Physician* **75**, 1523–1528 (2007).
- L. S. Alvord, B. L. Farmer, Anatomy and orientation of the human external ear. *J. Am. Acad. Audiol.* **8**, 383–390 (1997).
- CellsScope, <https://www.cellscope.com/> (2018).
- hearScope, <https://www.hearxgroup.com/hearscope/> (2018).
- R. Mandavia, T. Lapa, M. Smith, M. F. Bhutta, A cross-sectional evaluation of the validity of a smartphone otoscopy device in screening for ear disease in Nepal. *Clin. Otolaryngol.* **43**, 31–38 (2018).
- N. Erkkola-Anttinen, H. Irjala, M. K. Laine, P. A. Tähtinen, E. Löytyniemi, A. Ruohola, Smartphone otoscopy performed by parents. *Telemed. J. E-Health*, 10.1089/tmj.2018.0062 (2018).
- M. U. Shah, M. Sohal, T. A. Valdez, C. R. Grindle, iPhone otoscopes: Currently available, but reliable for tele-otoscopy in the hands of parents? *Int. J. Pediatr. Otorhinolaryngol.* **106**, 59–63 (2018).
- G. D. Hoople, Otitis media with effusion—A challenge to otolaryngology. *Laryngoscope* **60**, 315–329 (1950).
- M. E. Pichichero, Diagnostic accuracy, tympanocentesis training performance, and antibiotic selection by pediatric residents in management of otitis media. *Pediatrics* **110**, 1064–1070 (2002).
- A. Palmu, H. Puhakka, T. Rahko, A. K. Takala, Diagnostic value of tympanometry in infants in clinical practice. *Int. J. Pediatr. Otorhinolaryngol.* **49**, 207–213 (1999).
- R. Stoessel, N. Krohn, K. Pfeleiderer, G. Busse, Air-coupled ultrasound inspection of various materials. *Ultrasonics* **40**, 159–163 (2002).
- R. H. Wilson, K. P. Nadeau, F. B. Jaworski, B. J. Tromberg, A. J. Durkin, Review of shortwave infrared spectroscopy and imaging methods for biological tissue characterization. *J. Biomed. Opt.* **20**, 030901 (2015).
- A. F. Fercher, W. Drexler, C. K. Hitzenberger, T. Lasser, Optical coherence tomography - principles and applications. *Rep. Prog. Phys.* **66**, 239–303 (2003).
- P. H. Karma, M. A. Penttilä, M. M. Sipilä, M. J. Katja, Otoscopic diagnosis of middle ear effusion in acute and non-acute otitis media. I. the value of different otoscopic findings. *Int. J. Pediatr. Otorhinolaryngol.* **17**, 37–49 (1989).
- D. H. Keefe, J. C. Bulen, K. H. Arehart, E. M. Burns, Ear-canal impedance and reflection coefficient in human infants and adults. *J. Acoust. Soc. Am.* **94**, 2617–2638 (1993).
- H. Y. Lee, M. S. Choi, N. S. Park, C. S. Cho, Applicability of spectral gradient acoustic reflectometry (EarCheck): Screening patients who need surgical treatment for chronic otitis media with effusion. *Int. J. Pediatr. Otorhinolaryngol.* **78**, 107–111 (2014).

**Acknowledgments:** We thank our participants and their families at Seattle Children's Hospital for their willingness to participate in our study. We would like to acknowledge S. Parikh, J. Perkins, H. Thomas, H. Ou, J. Dahl, D. Horn, and K. Johnson for permitting us to recruit their patients and contributing data to the study. We would like to thank the Department of Pediatric Otolaryngology at the University of Washington as well as the operating room staff and personnel at Seattle Children's Hospital, especially at Seattle Children's Bellevue Clinic and Surgery Center, for enabling and facilitating patient recruitment. We thank K. Sie, C. Heike, J. Sunshine, E. Bly, S. Kaplan, V. Iyer, A. Wang, H. Shen, E. Wang, and S. Ainsworth for their critical and important feedback on the manuscript and methods. **Funding:** This study was supported by the NSF, the NIH, and the Seattle Children's Sie-Hatsukami Research Endowment. **Author contributions:** S.R., J.C., R.B., and S.G. designed the experiments; S.R. and J.C. conducted the experiments; J.C. and R.N. developed software and deployed the algorithm; S.R. and J.C. conducted the analysis; S.R., J.C., and R.N. interpreted results; J.C. generated figures; S.R., J.C., and S.G. wrote the manuscript; R.N. and R.B. edited the manuscript. Conceptualization: S.R. **Competing interests:** All co-authors are inventors on U.S. provisional patent application no. 62/72,8543, submitted by the University of Washington, which is related to this work. J.C., S.R., R.B., and S.G. have equity stakes in Edus Health Inc., which is related to the technology presented in this manuscript. S.G. is a cofounder of Jeeva Wireless Inc. and Sound Life Sciences Inc. R.B. is a consultant for SpiWay LLC and a cofounder of EigenHealth Inc. **Data and materials availability:** All data necessary for interpreting the manuscript have been included. Code is available with a noncommercial license; contact license@uw.edu.

Submitted 23 August 2018

Resubmitted 15 February 2019

Accepted 12 April 2019

Published 15 May 2019

10.1126/scitranslmed.aav1102

**Citation:** J. Chan, S. Raju, R. Nandakumar, R. Bly, S. Gollakota, Detecting middle ear fluid using smartphones. *Sci. Transl. Med.* **11**, eaav1102 (2019).

## Detecting middle ear fluid using smartphones

Justin Chan, Sharat Raju, Rajalakshmi Nandakumar, Randall Bly and Shyamnath Gollakota

*Sci Transl Med* **11**, eaav1102.  
DOI: 10.1126/scitranslmed.aav1102

### Hearing an ear infection?

Ear infections are typically diagnosed using specialized equipment to assess eardrum mobility: The presence of fluid in the middle ear, indicative of likely ear infection, limits eardrum mobility. Chan *et al.* developed a smartphone system to detect middle ear fluid that uses the microphone and speaker of a phone to emit sound and analyze its reflection (echo) from the eardrum. The smartphone system outperformed a commercial acoustic reflectometry system in detecting middle ear fluid in 98 pediatric patient ears, and the system could be easily operated by patient parents without formal medical training. This proof-of-concept screening tool could help aid in the diagnosis of ear infections.

#### ARTICLE TOOLS

<http://stm.sciencemag.org/content/11/492/eaav1102>

#### SUPPLEMENTARY MATERIALS

<http://stm.sciencemag.org/content/suppl/2019/05/13/11.492.eaav1102.DC1>

#### RELATED CONTENT

<http://stm.sciencemag.org/content/scitransmed/11/474/eaau8914.full>  
<http://stm.sciencemag.org/content/scitransmed/11/482/eaao0935.full>  
<http://stm.sciencemag.org/content/scitransmed/7/298/298ra118.full>

#### REFERENCES

This article cites 29 articles, 3 of which you can access for free  
<http://stm.sciencemag.org/content/11/492/eaav1102#BIBL>

#### PERMISSIONS

<http://www.sciencemag.org/help/reprints-and-permissions>

Use of this article is subject to the [Terms of Service](#)

*Science Translational Medicine* (ISSN 1946-6242) is published by the American Association for the Advancement of Science, 1200 New York Avenue NW, Washington, DC 20005. The title *Science Translational Medicine* is a registered trademark of AAAS.

Copyright © 2019 The Authors, some rights reserved; exclusive licensee American Association for the Advancement of Science. No claim to original U.S. Government Works